# Specific ratio of A- to B-type wheat starch granules improves the quality of gluten-free breads: optimizing dough viscosity and Pickering stabilization

Laura Román[1], Eva de la Cal[1], Manuel Gómez[1], Mario M. Martínez[2,3*]

[1]Food Technology Area. College of Agricultural Engineering, University of Valladolid, Palencia 34004, Spain.

[2]School of Engineering, University of Guelph, Guelph, Ontario N1G 2W1, Canada.

[3]Department of Food Science, University of Guelph, Guelph, Ontario N1G 2W1, Canada.

*Corresponding author e-mail: mario.martinez@uoguelph.ca

## Abstract

Specific volume and crumb hardness, cohesiveness and porosity of gluten-free breads (GFBs) are still far from consumers' expectations. Since additives are increasingly avoided by the consumers, a quality improvement of GFBs through the optimization of the starch source may provide important benefits. In this study, the effect of five different A- to B-type wheat starch ratios (100A-0B, 75A-25B, 50A-50B, 25A-75B, 0A-100B) on the quality of GFBs was investigated. The increase of the proportion of B-type granules (small ones) augmented the packing degree and uniformity of the continuous phase (starch-hydrocolloid matrix) as well as the Pickering effect (B-type granules being adsorbed onto the air-liquid interface), improving air bubble stabilization. In addition, 0A-100B dough displayed a more delayed crumb settling due to the higher pasting temperatures of B-type granules. Furthermore, the increase of the proportion of B-type granules also increased the apparent viscosity and viscoelastic moduli of doughs, which noticeable diminished bread expansion in 0A-100B sample. Interestingly, 75A-25B and 25A-75B doughs resulted in GFBs with the highest specific volume and crumb cohesiveness and lower crumb hardness, the former with open grain structure (fewer cells with larger size) and the latter with close grain structure (more cells with smaller size). For the first time, it is shown that a specific A- to B-type wheat starch ratio enables: 1) the simultaneous optimization of dough viscosity and Pickering stabilization to attain GFBs with improved physical quality and; 2) the modification of crumb porosity while maintaining specific volume and crumb texture.

Keywords: starch; gluten-free; bread; rheology; wheat; Pickering effect

## 1 Introduction

Consumers of gluten-free breads (GFBs) demand products with acceptable quality parameters. Since the gluten polymeric glutenins (the high molecular weight glutenin subunits) are critically responsible for elasticity and strengthening the dough (Shewry, Halford, Belton & Tatham, 2002), attaining elastic and resilient gluten-free crumbs still remains a major technological challenge. However, other quality parameters including the specific volume, crumb hardness, cohesiveness and porosity are the target of many "gluten-free" research groups, whose main tools mainly fall into two categories: the use of hydrocolloids and the optimization of the functionality of the starch fraction. Since additives are increasingly avoided by the consumers and partially contribute to the elevated price of gluten-free products, the improvement of GFB volume and texture with the optimization of the starch source is becoming of primary importance.

Many GFB recipes are mainly based on pure starches, where a combination of maize and potato is the most commonly used starchy composite, followed by the utilization of only maize starch or a mix of maize and another starch (Masure, Fierens & Delcour, 2016). However, the potential of wheat starch in gluten-free products remains unexplored, perhaps for the controversy over its actual safety. Although the allowance for its utilization depends on the country (Thompson, 2001), it has been proven that gluten-free wheat starch results in a similar histological and clinical recovery in coeliac patients than a natural gluten-free diet (Peräaho et al., 2003). In this way, guaranteed gluten-free wheat starch, containing less than 20 mg gluten/kg [legal limit for a product to be labelled as gluten-free according to the European Union regulations (Commission Regulation, 2009)], has appeared on the market.

Recent studies have shown a great potential of wheat starch for the production of gluten-free breads (Mancebo, Merino, Martinez & Gomez, 2015; Martinez & Gomez, 2017), which was attributed to its Pickering stabilization, multimodal particle size distribution (effect of small wheat starch granules filling the interstitial spaces of the big ones which reduced dough consistency) and water absorption capacity.

Stabilization of emulsion-based colloidal structures with mixed food ingredients, such as GFBs, has attracted attention (Binks & Murakami, 2006; Dickinson, 2012). Solid particles protect emulsion droplets against coalescence by being adsorbed onto the interface between the two phases. The Pickering emulsion, first reported in the early 20$^{th}$ century (Pickering, 1907; Ramsden, 1903), has gained renewed attention in the way that microparticles of biological origin, such as starch granules, work as stabilizers (Dickinson, 2012). Yano et al. (2017) experimentally evidenced Pickering stabilization of intact starch granules from rice flour as a mechanism to attain higher expansion of the dough/batter during fermentation and baking. Interestingly, in the same year, Martinez and Gomez (2017) also suggested a more pronounced Pickering stabilization of starch granules compared to flour particles, especially of the small wheat starch granules. However, there is no studies varying the ratio of small to large wheat granules to optimize Pickering and other stabilizing effects in GFB-making.

In mature wheat, two distinct classes of granules occur that differ in size and shape, i.e. large, lenticular (A-type) and small, spherical (B-type) granules. Quantitative separations of wheat starch granules followed by weighing indicated that wheat starch contains approximately 30% by weight of B granules (Maningat, Seib, Bassi, Woo & Lasater, 2009). Generally, A-type granules have higher amylose content and lower onset of gelatinization temperature, whereas B-type granules have higher lipid content and water absorption capacity (Guo, He, Xia, Qu & Zhang, 2014; Kim & Huber, 2010; Maningat et al., 2009; Soulaka & Morrison, 1985). Few studies have focused on the influence of varying the different A- to B-type starch ratio on the quality of gluten-containing breads, and results showed higher bread volumes with 25-35% B-type granules (Soulaka & Morrison, 1985; Park, Chung & Seib, 2005) and 60% B-type granules (Park et al., 2005). However, to the best of our knowledge, no studies of the influence on the A- to B-type wheat starch ratio on the quality of GFBs has been reported. We believe that different packing potential and Pickering synergies of the bimodal size distribution of wheat starch granules together with the different composition and physical properties of A- and B-type granules can give key knowledge on the quality improvement of GFBs.

In this way, five ratios of A- to B-type wheat starch granules (100A-0B, 75A-25B, 50A-50B, 25A-75B and 0A-100B) were obtained by combining A- and B-type commercial starches to bake GFBs. Dough structural and rheological properties were analyzed. Moreover, variations in bread structure, volume and degree of starch gelatinization as well as crumb texture were evaluated.

## 2. Materials and methods

### 2.1 Materials

Samples representing large (A-type) and small (B-type) wheat granules were gently supplied by AB Amilina (Panevezys, Lithuania), which is member of the group Roquette (Norte-Paso de Calais, France). Their starches, which contain mainly large and small wheat granules, are commercially termed A++ and A-, respectively. The granular size distribution can be observed in supplementary material 1 and mean diameter of equivalent volume d(4,3) is shown in Table 1. These two samples served as two commercially available representatives for A- and B-type wheat starch granules. It is noteworthy that ultrapure fractions are not commercially available because of limitations in the speed of industrial centrifuges for reasonable sized decanters, albeit they can be obtained in a laboratory scale.

Starch samples were characterized using AACC 76-31.01 method for damaged starch (AACC, 2015). Particle size was measured with a laser diffraction particle size analyzer (Mastersizer 3000, Malvern Instruments, Ltd., Worcestershire, UK). The mean diameter of equivalent volume d(4,3), which indicates the central point of the volume distribution of the particles, was recorded. Water binding capacity, defined as the amount of water retained by the starch after being subjected to centrifugation, was measured as described in the method 56-30.01 (AACC, 2015). Pasting properties were analyzed using the standard method 61-02.01 (AACC, 2015) with a Rapid Visco Analyzer (RVA-4) (Perten Instruments Australia, Macquarie Park, Australia). Thermal properties were analyzed following Roman, Gomez, Li, Hamaker and Martinez (2017) procedure using a differential scanning calorimeter Q-20 (TA instruments, Crawley, UK) equipped with a refrigerated cooling system (RCS 40). These analyses were carried out in duplicate.

The rest of ingredients were VIVAPUR 4KM HPMC (Hydroxypropyl Methylcellulose, JRS, Rosenberg, Germany), Saf-Instant dry yeast (Lesaffre, Lille, France), salt (Union Salinera de España, Madrid, Spain), sucrose (Azucarera, AB, Madrid, Spain), Abrilsol sunflower (Ourense, Spain) and tap water.

## 2.2 Methods

### 2.2.1 Dough preparation and bread-making

The starch fraction used for bread-making comprised five different A- to B-type wheat starch ratios, namely 100-0, 75-25, 50-50, 25-75 and 0-100. The rest of ingredients used were water (75 g/100 g starch), instant dry yeast (3 g/100 g), salt (2 g/100 g), oil (6 g/100 g), HPMC (2 g/100 g) and white sugar (5 g/100 g). Yeast was previously dissolved in water (at 20-22 $^{o}$C) before its incorporation. All the ingredients were mixed for 8 min in a Kitchen Aid 5KSM150 mixer (Kitchen Aid, Michigan, USA) with a flat beater (K45B) at speed 2. After kneading, 100 g of dough was placed in small aluminum moulds (140x40x35 cm, ALU-Schale, Wiklarn, Germany). Fermentation was performed at 30 °C and 90 % relative humidity for 90 min. Doughs were then baked in an electric modular oven for 40 min at 190 °C. Breads were cooled down for 30 min before storing them into sealed plastic aluminum bags in a temperature controlled chamber at 20 °C until further analysis. Bread-making was performed in duplicate.

2.2.2 Macro and microstructural analysis of doughs and breads

No yeast-containing doughs were observed with a DM750 optical microscope (Leica Microsystems, Wetzlar, Germany) fitted with an EC3 (for room temperature images) and Linkam video cameras (for hot-stage imaging). Room temperature and hot-stage images/videos were captured with LAS-EZ (Leica Microsystems, Wetzlar, Germany) and Link (Linkam Scientific Instruments Ltd, Waterfield, United Kingdom) software, respectively. Dough was placed on a glass microscope slide and covered with a cover slip. Then, sample slides were compressed under a 1 kg weight to create a layer of uniform thickness. Micrographs were taken at least twice in two random points of each sample.

Bread crumb and crust photomicrographs were taken with a Quanta 200FEI (Hillsboro, Oregon, USA) environmental scanning electron microscope (ESEM) in high vacuum mode. Crumb pictures were taken from a perpendicular slant to the cell wall highlighting the surface of the air cell wall. Conversely, crust pictures were taken showing their lengthwise section, i.e., showing the crust thickness. In order to better assess crumb macrostructure, bread slices were scanned in a HP Scanjet G3110 (Palo Alto, CA, USA).

### 2.2.3 Rheological properties of doughs

No yeast-containing doughs were covered with parafilm paper immediately after kneading and loaded into the rheometer at the earliest. Before conducting any rheological measurement, doughs were allowed to rest in the measurement position for 10 min as equilibration time, i.e., the necessary time to allow the stresses induced during sample loading to relax. The required equilibration time was selected according to previous time sweep tests carried out within the linear region at 1 Hz and 25 °C during 30 min. The time sweep test showed that in approximately 10 min, the values of G' and G" did not vary significantly with time (supplementary material 2). After adjustment of the gap, the exposed edges of the dough samples were always covered with vaseline oil (Panreac Quimica S.A., Castellar del Valles, Spain) to avoid sample drying during measurements. All rheological tests were run in duplicate in a controlled stress rheometer (Haake RheoStress 1, Thermo Fischer Scientific, Scheverte, Germany) with a titanium parallel plate geometry sensor PP60 Ti (60 mm diameter and 3 mm gap).

2.2.3.1 Viscoelastic properties

Linear viscoelastic properties were studied by small amplitude oscillatory test (SAOS). Dynamic linear viscoelastic range was estimated by performing a stress sweep from 0.1 to 50 Pa at 1 Hz frequency. Frequency dependence experiments were conducted from 10 to 0.01 Hz at 25 ºC. The applied stress (ranging from 0.15 to 0.60 Pa) was always selected to guarantee the existence of linear viscoelastic response. At least two replicates of each oscillatory shear test were conducted.

2.2.3.2. Flow properties.

Shear stress versus shear rate data was recorded using a titanium parallel plate geometry programmed to increase the shear stress from 1 to 150 Pa in step mode (30 seconds per point). Data was fitted to the Ostwald-de Waele model ($\sigma = K.\dot{\gamma}^n$), where σ is the shear stress (Pa), $\dot{\gamma}$ is the shear rate ($s^{-1}$), K is the consistency coefficient ($Pa.s^n$), and n is the flow behavior index (dimensionless). In this model, the apparent viscosity (η) can be calculated as ($\eta = K.\dot{\gamma}^{n-1}$). All measurements were made in duplicate.

### 2.2.4 Dough development and gas production

The dough development and gas production were recorded following the procedure previously described by Czuchajowska and Pomeranz (1993) using a rheofermentometer (Chopin, Villeneuve-la-Garenne, France). In contrast to the traditional method, the weight of dough was reduced to 200 g and the weights were removed from the piston due to the weakness of gluten-free dough compared to those prepared with wheat flour (Mancebo et al., 2015).

### 2.2.5 Physical properties of breads

Bread properties were evaluated 24 h after baking. Bread volume was determined using a laser sensor with the Volscan Profiler (Stable Micro Systems, Godalming, United Kingdom). Specific volume was calculated as the ratio of bread volume to its mass. Moisture loss (%) was calculated as the weight difference of the bread before and after baking process. The volume and moisture loss measurements were performed on two loaves from each batch.

Crumb texture was measured with a TA-XT2 texture analyzer (Stable Microsystems, Surrey, UK) equipped with the "Texture Expert" software. A 25-mm diameter cylindrical aluminum probe was used in a "Texture Profile Analysis" (TPA) double-compression test to penetrate up to 50% of the sample depth at a test speed of 2 mm/s, with a 30 s delay between the two compressions. Hardness (N), elasticity and cohesiveness were calculated from the TPA curve. Texture analyses were performed on 20 mm thickness central slices. Analyses were performed on two slices from two loaves from each formulation.

### 2.2.6 Thermal analysis in bread crumb and crust

The degree of starch gelatinization in bread crumb and crust was analyzed with a differential scanning calorimeter (DSC) Q-20 (TA instruments, Crawley, UK) equipped with a refrigerated cooling system (RCS 40) as reported in Martinez, Roman and Gomez (2018). Briefly, freeze-dried dough, crumb (middle of the central slice) and crust (scratched surface) samples were mixed in a 1:2 ratio (w/w) with water and hermetically sealed in Tzero hermetic aluminum DSC pans. An empty pan was used as reference. Samples were kept at 30 ºC for 30 min and heated from 30 to 110 ºC at 10 ºC/min.

The degree of gelatinization was calculated based on the enthalpy values of gelatinization as follows:

$$\text{Gelatinization degree (\%)} = \left(1 - \frac{\Delta HD}{\Delta HB}\right) * 100$$

Where $\Delta H_D$ is the enthalpy of a portion of dough and $\Delta H_B$ is the enthalpy of crumb or crust samples, respectively. Each dough, crumb and crust sample for each elaboration was run in triplicate.

### 2.2.7 Statistical analysis

Differences between the parameters for the doughs and breads were studied by analysis of variance (ANOVA). Fisher's least significant difference (LSD) was used to describe means with 95% confidence intervals. The statistical analysis was performed with Statgraphics Centurion XVI software (Statpoint Technologies, Inc., Warrenton, USA).

## 3 Results and discussion

### 3.1 Doughs microstructure

Optical microscopy (Fig. 1) revealed the packing of starch granules after mixing. In all micrographs (A-E), the different starch granules appeared forming a continuous phase (liquid phase) surrounding gas bubbles (large and spherical cells pointed with arrows). This continuous phase became more uniform as the proportion of in B-type starch increased, likely because of the better packing capability of the small and spherical B-type wheat granules. On the other hand, doughs with a high ratio of A-type starch granules exhibited a less packed granular conformation and non-uniform continuous phase (more empty interstitial spaces) due to the larger size and lenticular form of A-type granules. Similarly, Martinez and Gomez (2017) reported a less compact granular conformation in gluten-free doughs made with potato starch (with equivalent diameter of ~45µm), one of the largest starch granules found in plant tissues. Furthermore, the same authors showed that, in doughs containing wheat starch granules with bimodal particle size distribution (samples containing starch granule populations with marked differences in size), the small granules (B-type) filled the interstitial spaces of the large ones (A-type), which extensively affects the rheological properties of the dough system and bread quality.

Gas bubbles, which form the discontinuous phase (gaseous phase) in the dough system, are embedded in the matrix composed by starch granules and HPMC. Since gas bubbles can potentially be mistaken by large A-type granules in the micrographs due to their size and shape, differences in the amount of incorporated air were not clearly visible among samples, although apparently 0A-100B displayed smaller air bubbles compared to 100A-0B. Air bubbles were surrounded by wheat starch granules, with only B-type granules being adsorbed onto the interface, especially as its proportion increased (Fig. 1F). It is known that microparticles, such as starch granules, work as stabilizers. In particular, Dickinson (2012) stated that these solid particles in the continuous phase would be adsorbed at the gas-aqueous phase interface to form a barrier protecting droplets against coalescence, which is known as Pickering stabilization. However, in order for adsorbed particles to achieve effective Pickering stabilization, their average size should be at least an order of magnitude smaller than the emulsion droplet size. Therefore, it seems that 5-15µm particles are needed to stabilize 50-150µm air droplets. Pickering stabilization in gluten-free rice doughs was also reported by Yano et al. (2017), who showed a surface of air bubbles covered by 5 µm rice starch granules, similar in size to the B-type wheat starch granules used in the present study (6.09 µm, see Table 1). In fact, these authors attributed the feasibility to make rice breads to the Pickering stabilization property of rice starch granules.

Dough microstructure after heating up to 100 $^{o}$C also revealed a noticeable different behavior of doughs (Fig. 2). In particular, air bubbles in 0A-100B sample better preserved their rounded morphology while a distorted bubble shape and bubble coalescence were observed in 100A-0B. It is believed that this event may be the result of B-type granules being adsorbed onto the gas-aqueous phase interface (Pickering stabilization). A movie during heating from 30 to 100 $^{o}$C is also shown in supplementary material 3. During heating, both 100A-0B and 0A-100B doughs exhibited gradual swelling and gelatinization of starch granules and crumb settling. However, 0A-100B dough displayed a more delayed crumb settling due to the higher gelatinization and pasting temperatures of B-type granules (Table 1).

**3.2 Dough rheological properties.**

3.2.1 Viscoelastic properties.

In the analyzed frequency range, all samples exhibited G' higher than G", with both moduli depending on frequency but following a different pattern (Fig. 2). This region, called the plateau relaxation zone, has already been observed for gluten-free doughs made with different starches (Martinez et al., 2015) and it is characterized by the occurrence of physical entanglements among the different polymeric materials (Ferry, 1980). Starch-based gluten-free doughs mainly consist on few air bubbles (generated mainly during kneading) surrounded by a continuous phase (network) composed by starch granules and hydrocolloid (Fig. 1, Martinez & Gomez, 2017). Higher viscoelastic moduli were observed as the proportion of B-type granules increased in the formula. Chiotelli and Le Meste (2002) also observed higher G’ of B-type starch dispersions in water at room temperature compared to A-type based-counterparts. Other authors reported that B-type wheat starch granules have higher water-binding capacity and affinity for water than A-type counterparts, which was attributed to the higher specific surface area of the former (Chiotelli & Le Meste, 2002; Guo et al., 2014; Park et al., 2005). This is supported by data shown in Table 1, where B-type granules possessed higher water absorption capacity, likely due not only to their higher surface area but also to their higher damaged starch content (Table 1), which has been suggested to be located at the periphery of the granules (Roman et al., 2017). In fact, native wheat starch can only hold 0.3-0.45 g of water per gram of dry starch, whereas damaged starch (produced by milling) can hold 1.5-2 g of water per gram of dry starch (Kweon, Slade & Levine, 2011). Another explanation for the higher consistency of B-type starch-based doughs may be related to the effect of their size and shape on creating a more continuous liquid phase and stabilizing air bubbles. Firstly, small spherical granules (B-type) would easily pack up to result in a more closely packed continuous phase with less discontinuities in the hydrocolloid network compared to that from A-type granules. Secondly, since typically higher values of viscoelastic moduli are found in dispersions with highly packed droplets, a better stabilization of the gaseous phase might be also occurring in doughs containing B-type granules because of their noticeable Pickering stabilization. All these physical occurrences would also be supported by the lower loss tangent values in B-type starch-based doughs, indicating higher dough elasticity (Table 2). These hypotheses would align with the results found by Ma and Barbosa-Canovas, (1995), who reported higher values of viscoelastic moduli in dispersions with droplets highly packed (smaller and more abundant bubbles).

3.2.2 Dough flow behavior.

The apparent viscosity at 0.001 $s^{-1}$ [typical shear rate of dough expansion during fermentation, (Menjivar, 1990)] was calculated from the Ostwald-de Waele model and shown in Table 2. Dough consistency and apparent viscosity were both measured as complimentary rheological techniques with different stress. Specifically, the stress applied during the steady flow analysis is significantly higher and outside the linear viscoelastic region (LVR), which gives additional information about the interaction among the different components (considered as different rheological units). The flow curves revealed the shear thinning behavior (decrease in apparent viscosity as shear rate increases), mainly attributed to the alignments of starch granules and breakdown of the network formed between the granules under the influence of shear flow (data not shown). An increase in apparent viscosity was found as the proportion of B-type starch increased, which was in accordance with the trend found for the viscoelastic moduli (although in this case, no significant differences were found between 100A-0B, 75A-25B, and 50A-50B). The increase of apparent viscosity from 9354 Pa.s in 25A-75B to 23744 Pa.s in 0A-100B is worthy of mentions. This could be attributed to 1) the greater packing ability of small and rounded starch granules leading to a more closely packed granular conformation and strongly bound continuous phase (starch-hydrocolloid matrix) and; 2) the higher water binding capacity of small granules (higher water uptake). As regard to the latter, there might be a competition of starch granules for the water available, which seems to become limited from a 75 % B-type proportion (the ones with higher water absorption capacity). Albeit, the dough continuous phase is a concentrated system of starch granules that are in close proximity, it does not fit proposed models showing the apparent viscosity as a strong positive function of the volume fraction of the particle ($\phi$) and a negative function of the maximum packing volume fraction ($\phi_m$, defined as the maximum number of particles that can be packed in a given volume) (Farris, 1968; Schneider et al. 2002; Servais, Jones & Roberts, 2002). These models were proposed for non-interacting multimodal spherical particles (i.e. different populations differing in size), and in the dough system, particles are interacting non-spherical particles that absorb water and swell, resulting in an even more complex system to investigate.

3.2.3 Rheofermentometic analysis.

The gas production during fermentation showed no differences among samples (supplementary material 4), although 100A-0B exhibited slightly lower gas production at the beginning of the curve likely because of the lower damage starch of A-type wheat starch. In all cases, a decrease in gas production at around 120 min was observed, indicating a complete consumption of fermentable sugars by the yeast after 2 h of fermentation (Mancebo et al., 2015). Analyses of dough development were not performed successfully because of the low consistency of some of the doughs (the least consistent/viscous doughs, namely 100A-0B, 75A-25B and 50A-50B), which overflowed when the piston was assembled (data not shown), leading to an inaccurate recording of results.

### 3.3 Macro and micro-scale structure and degree of starch gelatinization of bread

The structure of bread crumb is exhibited in Fig. 3A. As the proportion of A-type wheat starch increased, fewer cells with larger cell size were observed, whereas small wheat granules (B-type) resulted in crumbs with greater number of cells with smaller size. Albeit the cell size increased with the presence of large starch granules, 75A-25B sample exhibited the most open grain structure. In 1988, Hayman, Sipes, Hoseney and Faubion, reported that starch size is an important factor affecting crumb grain structure. These authors observed that the presence of a greater proportion of large starch granules in wheat flour dough was sufficient to result in gas cell coalescence and open crumb grain. It can be assumed that this occurrence is due to the Pickering stabilization of small wheat starch granules (B-type), which may be adsorbed onto the gaseous-liquid interphase and stabilize gas cells by reducing their interfacial tension, preventing coalescence, and forming a closer crumb grain. Furthermore, the higher consistency of B-type-based doughs (see section 3.2) could also contribute to prevent the coalescence phenomena of gas bubbles. Added to that, a closer look at the gas cell walls (perpendicular slant, Fig. 3B) revealed the presence of some starch granules in B-type-based crumbs, whereas the contour of starch granules completely disappeared for A-type crumbs. When reaching a certain temperature, the hydrated starch gelatinizes, leading to crumb settling (Le-Bail et al., 2011), and, thus, forming the grain structure that covers the gas cells. These results are supported by RVA and DSC data (Table 1), where B-type wheat starch granules exhibited higher onset temperature of gelatinization ($T_o$) and pasting temperature (PT). In fact, Chiotelli and Le Meste (2002) indicated that heated swollen B-type granules were somewhat less deformable than A-type granules during cooling. This is an important factor since those swollen starch granules that better preserve their morphology could influence positively the structure of the continuous (liquid) phase. For better comprehension, B-type granules could be seen as the “bricks” and the mass of hydrocolloid and melted A-type granules as the cement, which together would define the walls surrounding the room space (in this case, the gas bubbles).

Interestingly, the degree of starch gelatinization in bread crumb, analyzed as the amount of amylopectin double helices remaining after baking (Martinez, Roman & Gomez, 2018), was equally complete in all samples (Table 3). These results would indicate that both A- and B-type wheat starch granules in crumb are completely gelatinized after baking. However, B-type granules, unlike A-type ones, resist disintegration and dispersion throughout the liquid phase. Crust samples underwent significantly less gelatinization during baking as the proportion of B-type granules increased, ranging from 15.18% in 0A-100B to 30.11% in 100A-0B (Table 3). These values are in agreement with those presented by Primo-Martín, van Nieuwenhuijzen, Hamer and van Vliet (2007) and Varriano-Marston, Ke, Huang and Ponte (1980). The fast evaporation of water from the crust due to the high temperature of the surface of the crust impairs the full gelatinization of the starch (Primo-Martín et al., 2007). In this case, the 2 $^{o}$C higher of the onset temperature of gelatinization for B-type wheat starch compared to the A-type counterpart (Table 1) seemed to be enough to significantly affect their resistance to gelatinize under the hydrothermal historic reached in the crust during baking.

### 3.4 Physical properties of breads

The specific volume of breads and the crumb textural properties are shown in Table 2. Only taking into account 100A-0B, 50A-50B and 0A-100B samples, a lower consistency and apparent viscosity were found to result in the most voluminous breads. This correlation has been previously reported by several authors (Lazaridou, Duta, Papageorgiou, Belc & Biliaderis, 2007; Mancebo et al., 2015; Martinez & Gomez, 2017; Rocha-Parra, Ribotta & Ferrero, 2015), which may be attributed to the higher damaged starch and surface area of B-type wheat granules that increases water absorption capacity and dough consistency (Fig. 2 and Table 2). This event could potentially halt the expansion of the gas cells during fermentation and baking. Interestingly, 75A-25B and 25A-75B bread samples exhibited the highest volume, which is in agreement with previous works on gluten-containing breads showing higher volumes with 25-35% B-type granules (Park et al., 2005; Soulaka & Morrison, 1985) and 60% B-type granules (Park et al., 2005). Soulaka and Morrison (1985) attributed this phenomenon to an optimum surface area achieved with 25-35% B-type wheat starch granules, whereas Park et al. (2005) related this event to an optimum demand of water. In the present work, not a single parameter that explains this occurrence was found, which exhibits again the complexity of the continuous phase. The reasons for the better volume of 75A-25B and 25A-75B might be related to synergistic factors including, differences in the degree and temperatures of the starch physical transitions during baking, water absorption capacity and dough viscosity/consistency and Pickering stabilization of the dispersed phase.

The specific volume of bread was inversely correlated with its hardness, defined as the peak force during the first compression cycle. This reciprocal relationship has been reported in previous studies (Gallagher, Gormley & Arendt, 2003; Martinez & Gomez, 2017; Martinez, Roman & Gomez, 2018). 75A-25B and 25A-75B samples exhibited crumbs with the most desirable textural properties (lower hardness and higher elasticity and cohesiveness). Cohesiveness, which quantifies the internal resistance or cohesion of crumb structure, and springiness, whose reduction has been associated with the loss of crumb elasticity (Onyango, Mutungi, Unbehend & Lindhauer, 2011), are positive attributes that consumers demand in a bread crumb.

## 4 Conclusions

Gluten-free breads (GFBs) with high specific volume and crumb cohesiveness and low hardness are preferable over hard and low volume loaves. In this work, it is shown that these parameters can be significantly improved by means of optimizing the A- to B-type wheat starch ratio. It seems that the proper proportion of starch granules varying in particle size, surface area, swelling capacity and resistance to lose their semi-crystalline structure and morphology during baking may empower the continuous phase with a combined rigidity and support (from B-type granules) and continuity and flowability (from melted A-type granules) that results in optimum crumb settling during baking. In particular, 75A-25B dough would possess a low apparent viscosity with enough number of B-type granules to improve Pickering stabilization. On the other hand, 25A-75B dough would benefit from a larger number of B-type granules providing Pickering stabilization and a robust structure that would become cohesive with the presence of fully melted A-type granules. Results also suggest that a proportion of 50% of each population does not reach the optimum equilibrium of the aforementioned conditions to obtain breads with improved physical properties.

Results of this work would also suggest that the unique physical and sensory quality of wheat breads is not only due to the presence of gluten, but also to the proper A- to B-type starch ratio (~70% in native wheat flour) that result in the optimum physical properties of the continuous phase from a carbohydrate standpoint.

**Acknowledgments**

The authors acknowledge the financial support of the Spanish Ministry of Economy and Competitiveness (Project AGL2014-52928-C2) and the European Regional Development Fund (FEDER). Laura Roman would like to thank the University of Valladolid for her pre-doctoral fellowship. The authors are grateful to Roquette for supplying the raw materials.

**References**

AACC (2015). Approved methods of the American Association of Cereal Chemists, Methods 76-31.01 (damaged starch), 56-30.01 (water binding capacity), 61-02.01 (rapid visco analysis), 11th ed. American Association of Cereal Chemists, St. Paul, Minnesota.

Binks, B. P., & Murakami, R. (2006). Phase inversion of particle-stabilized materials from foams to dry water. *Nature Materials,* 5, 865-869.

Chiotelli, E., & Le Meste, M. (2002). Effect of small and large wheat starch granules on thermomechanical behavior of starch. *Cereal Chemistry,* 79, 286-293.

Commission Regulation (EC) No. 41/2009. Article 3: Composition and labelling of foodstuffs for people intolerant to gluten.

Czuchajowska, Z., & Pomeranz, Y. (1993). Gas-formation and gas retention. 1. The system and methodology. *Cereal Foods World*, 38, 499-503.

Dickinson, E. (2012). Use of nanoparticles and microparticles in the formation and stabilization of food emulsions. *Trends in Food Science and Technology*, 24, 4-12.

Farris, R.J. (1968). Prediction of the viscosity of multimodal suspensions from unimodal viscosity data. *Transactions of the Society of Rheology*, 12, 281-301.

Ferry, J.D. (1980). *Viscoelastic Properties of Polymers*. (3rd ed.). John Wiley & Sons Inc, New York.

Gallagher, E., Gormley, T.R., & Arendt, E.K. (2003). Crust and crumb characteristics of gluten-free breads. *Journal of Food Engineering*, 56, 153-161.

Guo, Q., He, Z., Xia, X., Qu, Y., & Zhang, Y. (2014). Effects of wheat starch granule size distribution on qualities of Chinese steamed bread and raw white noodles. *Cereal Chemistry*, 91, 623-630.

Hayman, D., Sipes, K., Hoseney, R. C., & Faubion, J. M. (1998). Factors controlling gas cell failure in bread dough. *Cereal Chemistry*, 75, 585-589.

Kim, H. S., & Huber, K. C. (2010). Physicochemical properties and amylopectin fine structures of A- and B-type granules of waxy and normal soft wheat starch. *Journal of Cereal Science*, 51,256-264.

Kweon, M., Slade, L., & Levine, H. (2011). Solvent retention capacity (SRC) testing of wheat flour: principles and value in predicting flour functionality in different wheat-based food processes and in wheat breeding-a review. *Cereal Chemistry*, 88, 537-552.

Lazaridou, A., Duta, D., Papageorgiou, M., Belc, N., & Biliaderis, C. G. (2007). Effects of hydrocolloids on dough rheology and bread quality parameters in gluten-free formulations. *Journal of Food Engineering*, 79, 1033-1047.

Le-Bail, A., Dessev, T., Leray, D., Lucas, T., Mariani, S., Mottollese, G., & Jury, V. (2011). Influence of the amount of steaming during baking on the kinetic of heating and on selected quality attributes of bread. *Journal of Food Engineering*, 105, 379-385.

Lin, Y.S., Yeh, A.I., & Lii, C.Y. (2001). Correlation between starch retrogradation and water mobility as determined by differential scanning calorimetry (DSC) and nuclear magnetic resonance (NMR). *Cereal Chemistry*, 78, 647–653.

Ma, L., & Barbosa-Canovas, G. V. (1995). Rheological characterization of mayonnaise. Part II: Flow and viscoelastic properties at different oil and xanthan gum concentrations. *Journal of Food Engineering*, 25, 409-425.

Mancebo, C. M., Merino, C., Martínez, M. M., & Gómez, M. (2015). Mixture design of rice flour, maize starch and wheat starch for optimization of gluten free bread quality. *Journal of Food Science and Technology*, 52, 6323-6333.

Maningat, C. C., Seib, P. A., Bassi, S. D., Woo, K. S., & Lasater, G. D. (2009). Wheat Starch: Production, Properties, Modification and Uses. In: J. BeMiller, & R. Whistler (Eds.). *Starch. Chemistry and Technology*. (pp. 441-510). New York: Academic Press.

Martinez, M. M., & Gómez, M. (2017). Rheological and microstructural evolution of the most common gluten-free flours and starches during bread fermentation and baking. *Journal of Food Engineering*, 197, 78-86.

Martinez, M. M., Roman, L. & Gómez, M. (2018). Implications of hydration depletion in the in vitro starch digestibility of white bread crumb and crust. *Food Chemistry*, 239, 295-303.

Martinez, M.M., Sanz, T., & Gomez, M. (2015). Influence of wheat flour subjected to different extrusion conditions on the rheological behaviour and thermal properties of batter systems for coating. *LWT-Food Science and Technology*, 64, 1309-1314.

Masure, H. G., Fierens, E., & Delcour, J. A. (2016). Current and forward looking experimental approaches in gluten-free bread making research. *Journal of Cereal Science*, 67, 92-111.

Menjivar, J.A. (1990). Fundamental aspects of dough rheology. In: H. Faridi & J. M. Faubion (Eds.). *Dough rheology and baked product texture*. (pp. 1-28). AVI Publishing, New York, USA.

Onyango, C., Mutungi, C., Unbehend, G., & Lindhauer, M. G. (2011). Modification of gluten-free sorghum batter and bread using maize, potato, cassava or rice starch. *LWT-Food Science and Technology*, 44, 681-686.

Park, S.-H., Chung, O. K., & Seib, P. A. (2005). Effects of varying weight ratios of large and small wheat starch granules on experimental straight-dough bread. *Cereal Chemistry*, 82, 166-172.

Peräaho, M., Kaukinen, K., Paasikivi, K., Sievänen, H., Lohiniemi, S., Mäki, M., & Collin, P (2003). Wheat-starch-based gluten-free products in the treatment of newly detected coeliac disease: prospective and randomized study. *Alimentary Pharmacology & Therapeutics*, 17, 587-594.

Pickering, S. U. (1907). Emulsions. *Journal of the Chemical Society, Transactions*, 91, 2001-2021.

Primo-Martín, C., van Nieuwenhuijzen, N. H., Hamer, R. J., & van Vliet, T. (2007). Crystallinity changes in wheat starch during the bread-making process: Starch crystallinity in the bread crust. *Journal of Cereal Science*, 45, 219-226.

Ramsden, W. (1903). Separation of solids in the surface-layers of solutions and suspensions. *Proceedings of the Royal Society of London*, 72, 156-154.

Rocha-Parra, A.F., Ribotta, P.D., Ferrero, C. (2015). Apple pomace in gluten-free formulations: effect on rheology and product quality. *International Journal of Food Science and Technology*, 50, 682-690.

Roman, L., Gomez, M., Li, C., Hamaker, B.R., & Martinez, M.M. (2017). Biophysical features of cereal endosperm that decrease starch digestibility. *Carbohydrate Polymers*, 165, 180-188.

Schirmer, M., Jekle, M., & Becker, T. (2015). Starch gelatinization and its complexity for analysis. *Starch-Stärke*, 67, 30-41.

Servais, C., Jones, R., & Roberts, I. (2002). The influence of particle size distribution on the processing of food. *Journal of Food Engineering*, 51, 201-208.

Shewry, P.R., Halford, N.G., Belton, P.S., & Tatham, A.S. (2002). The structure and properties of gluten: an elastic protein from wheat grain. Ph*ilosophical transactions of the Royal Society of London*, 357, 133-142.

Schneider, M., Claverie, J., Graillat, C., & McKenna, T. F. (2002). High solids content emulsions. I. A study of the influence of the particle size distribution and polymer concentration on viscosity. *Journal of Applied Polymer Science*, 84, 1878-1896.

Soulaka, A. B., & Morrison, W. R. (1985). The bread baking quality of six wheat starches differing in composition and physical properties. *Journal of the Science of Food and Agriculture*, 36, 719-727.

Thompson, T. (2001). Wheat starch, gliadin, and the gluten-free diet. *Journal of The American Dietetic Association*, 101, 1456-1459.

Varriano-Marston, E., Ke, V., Huang, G., & Ponte, J. (1980). Comparison of methods to determine starch gelatinization of bakery foods. *Cereal Chemistry*, 57, 242-248.

Yano, H., Fukui, A., Kajiwara, K., Kobayashi, I., Yoza, K. I., Satake, A., & Villeneuve, M. (2017). Development of gluten-free rice bread: Pickering stabilization as a possible batter-swelling mechanism. *LWT-Food Science and Technology*, 79, 632-639.

**Table 1**. Moisture and physical properties of A and B-type wheat starches.

| Sample | D(4,3) (μm) | DS (g/100g) | WBC (g water/ g solid) | PT (ºC) | PV (cP) | BR (cP) | SB (cP) | To (ºC) | Tp (ºC) | Tc (ºC) | $\Delta H_g$ (J/g) |
|---|---|---|---|---|---|---|---|---|---|---|---|
| A-type | 19.9 ± 0.5 | 1.40 ± 0.20 | 0.649 ± 0.009 | 69.8 ± 0.4 | 4682 ± 57 | 1258 ± 26 | 2130 ± 72 | 55.83 ± 0.02 | 61.50 ± 0.01 | 72.78 ± 0.21 | 7.65 ± 0.07 |
| B-type | 6.1 ± 0.3 | 2.78 ± 0.02 | 0.767 ± 0.001 | 89.4 ± 0.4 | 3107 ± 17 | 304 ± 7 | 1444 ± 87 | 57.39 ± 0.05 | 62.43±0.02 | 74.65 ± 1.12 | 7.69 ± 0.04 |

D(4,3), De Brouckere mean diameter; DS; damaged starch, WBC, water binding capacity; PT, pasting temperature; PV, peak viscosity; BR, breakdown; ST, setback, To, Tp and Tc indicates onset, peak and conclusion temperature of gelatinization; $\Delta H_g$, enthalpy of gelatinization.

**Table 2.** Effect of different ratios of A and B-type starches on loss tangent and apparent viscosity of dough and bread properties.

| Sample | tanδ | η (Pa·s) | Specific volume (mL/g) | Hardness (N) | Springiness | Cohesiveness |
|---|---|---|---|---|---|---|
| 100 A - 0 B | 0.776c ± 0.039 | 3939a ± 91 | 7.29b ± 0.67 | 1.21b ± 0.20 | 1.28ab ± 0.35 | 0.81a ± 0.02 |
| 75 A - 25 B | 0.702bc ± 0.070 | 4980a ± 461 | 8.28c ± 0.29 | 0.78a ± 0.19 | 1.82bc ± 0.77 | 0.82ab ± 0.03 |
| 50 A - 50 B | 0.657b ± 0.032 | 5504a ± 276 | 7.10b ± 0.38 | 1.08b ± 0.18 | 1.02a ± 0.10 | 0.81a ± 0.03 |
| 25 A - 75 B | 0.433a ± 0.016 | 9354b ± 323 | 8.12c ± 0.36 | 0.61a ± 0.07 | 2.01c ± 0.80 | 0.84b ± 0.02 |
| 0 A - 100 B | 0.412a ± 0.011 | 23744c ± 1335 | 6.02a ± 0.42 | 1.43c ± 0.14 | 0.98a ± 0.03 | 0.80a ± 0.01 |

Values followed by the same letters within each parameter indicate no significant differences ($p \leq 0.05$). tanδ, loss factor; η, apparent viscosity at 0.001 $s^{-1}$

**Table 3.** Degree of starch gelatinization of bread crumb and crust.

| | *Crumb* | *Crust* |
|---|---|---|
| | Degree of starch gelatinization (g gelatinized starch/100 g starch) | Degree of starch gelatinization (g gelatinized starch/100 g starch) |
| 100 A - 0 B | 100a ± 0.00 | 28.54 b ± 1.67 |
| 75 A - 25 B | 100a ± 0.00 | 28.43b ± 0.98 |
| 50 A - 50 B | 100a ± 0.00 | 30.11 b ± 2.26 |
| 25 A - 75 B | 100a ± 0.00 | 19.06 a ±2.66 |
| 0 A - 100 B | 100a ± 0.00 | 15.18a ± 0.13 |

Values followed by the same letters within each parameter indicate no significant differences (p≤0.05).

**Fig 1.** Optical micrographs of 100-0 (A), 75-25 (B), 50-50 (C), 25-75 (D) and 0-100 (E) ratios of A- to B-type wheat starch granules. (F) Higher magnification of 0A-100B dough showing B-type granules adsorbed onto the gas-aqueous interface. Arrows denote air bubbles in the doughs.

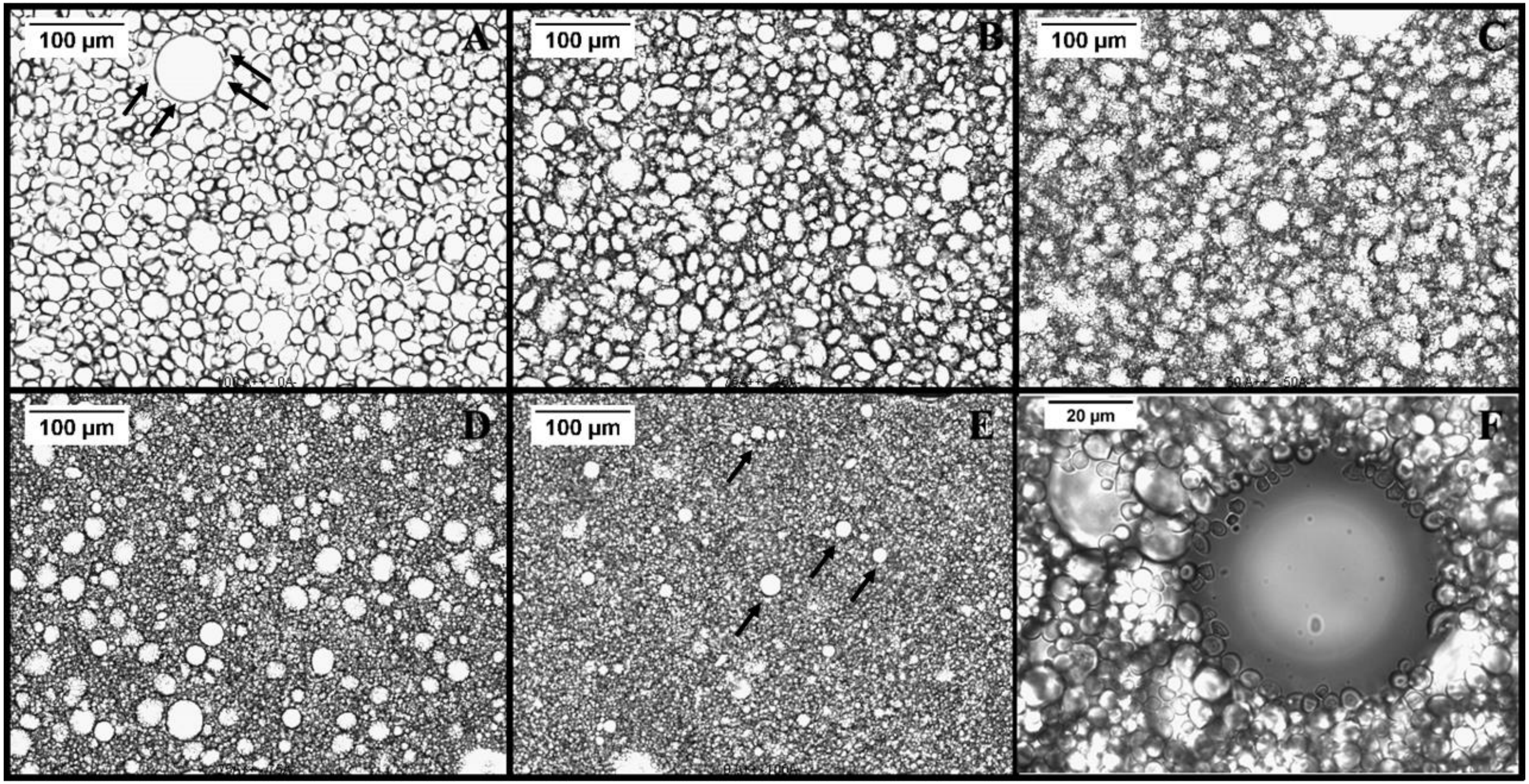

**Fig 2.** Optical micrographs of doughs made with 100-0 (A) and 0-100 (B) ratios of A- to B-type wheat starch granules highlighting different bubble shape preservation after dough heating.

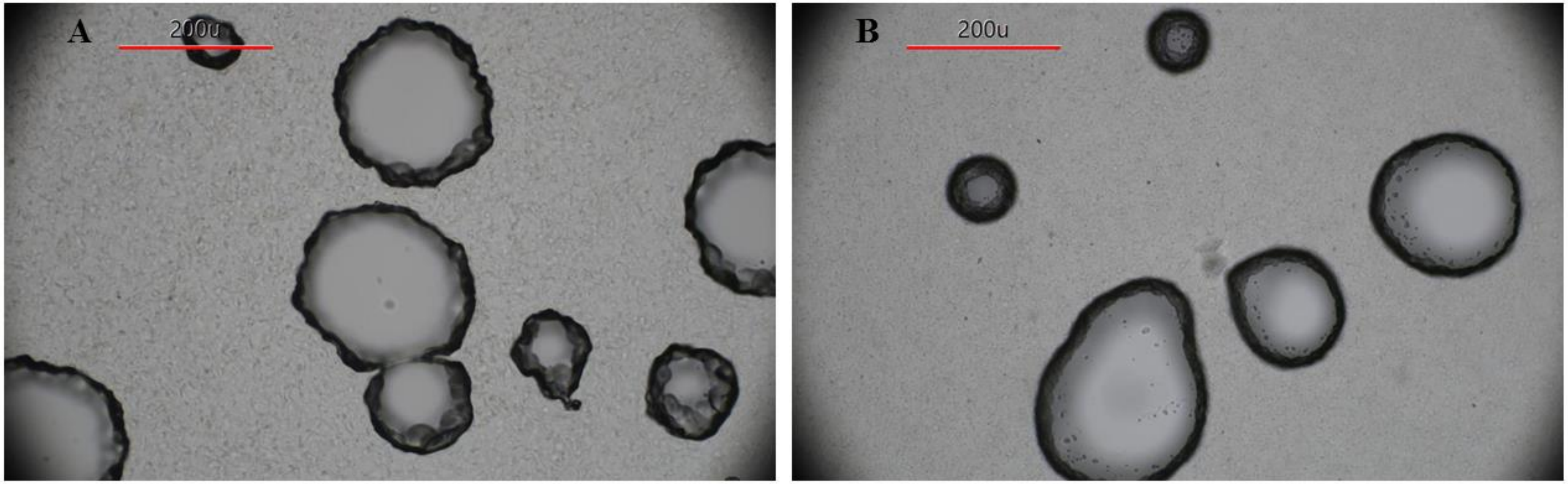

**Fig 3**. Mechanical spectra of doughs containing different ratios of A- to B-type wheat starch granules. 0A-100B (square) 25A-75B (triangle) 50A-50B (circle) 75A-25B (diamond) and 100A-0B (cross or dash). G' and G'' are displayed as filled and non-filled markers, respectively.

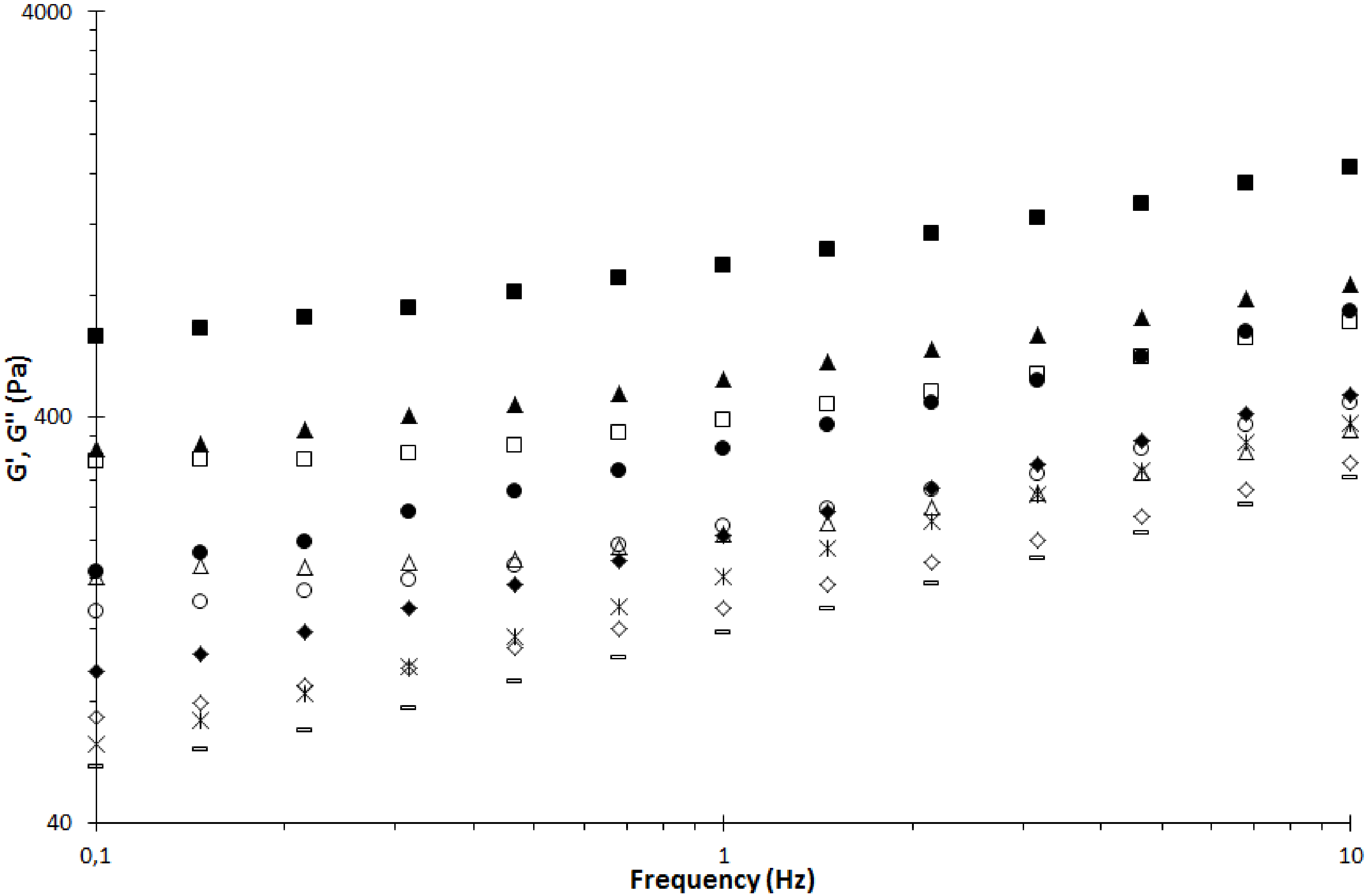

**Fig 4.** A: Crumb micrographs of breads made with 100-0, 75-25, 50-50, 25-75 and 0-100 ratios of A- to B-type wheat starch granules (left to right). B: Cell wall detail (perpendicular slant to cell wall) of crumbs made with 100-0 (left) and 0-100 (right) ratios of A- to B-type wheat starch granules.

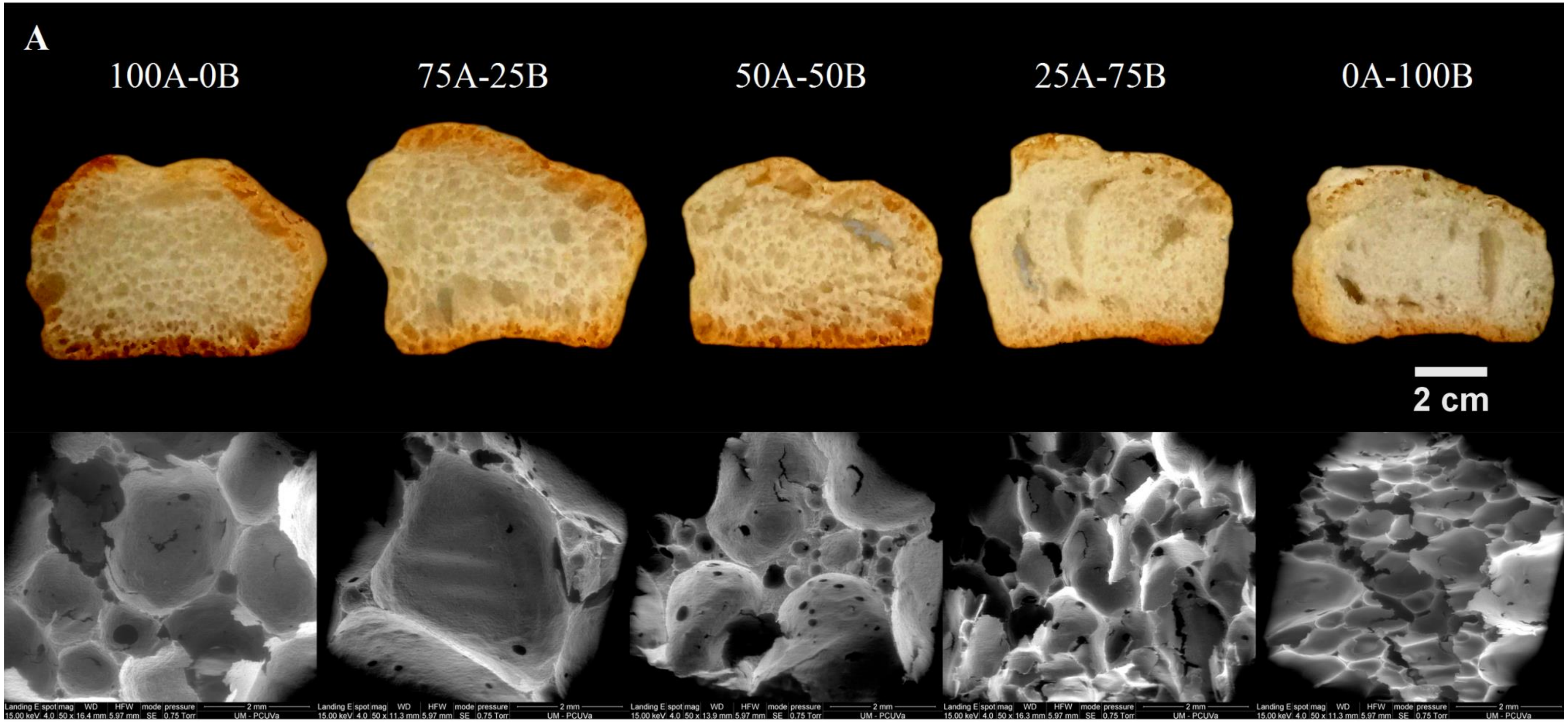

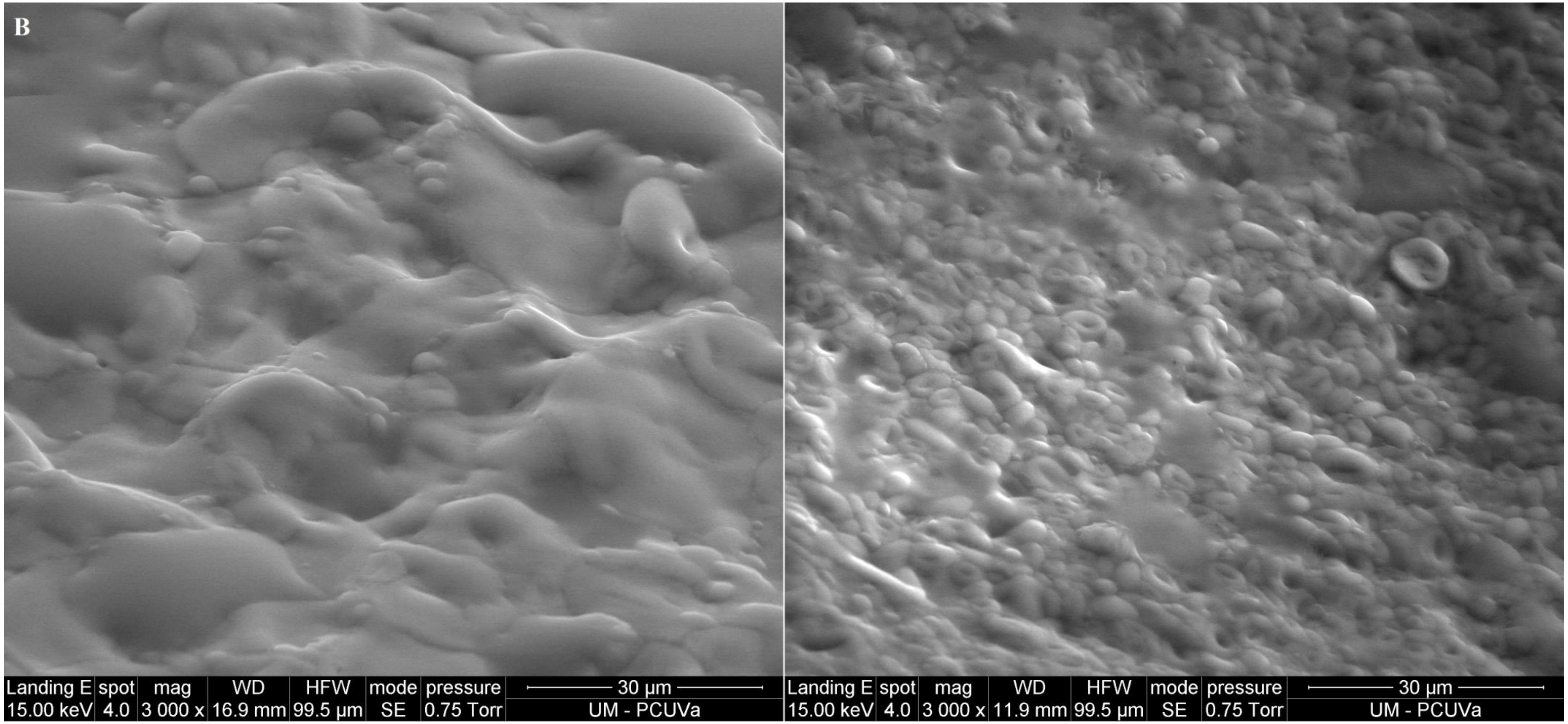
B
Landing E spot mag WD HFW mode pressure 30 µm
15.00 keV 4.0 3 000 x 16.9 mm 99.5 µm SE 0.75 Torr UM - PCUVa
Landing E spot mag WD HFW mode pressure 30 µm
15.00 keV 4.0 3 000 x 11.9 mm 99.5 µm SE 0.75 Torr UM - PCUVa

**Supplementary material**

Supplementary material 1. Particle size distribution of A- and B-type starch granules.

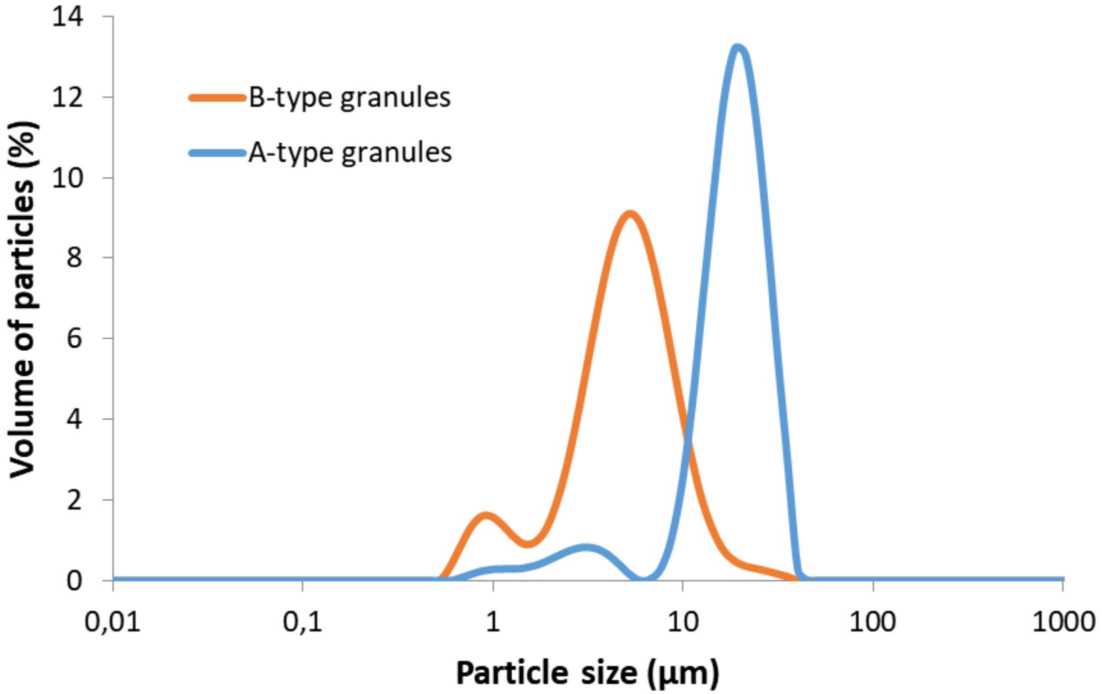

Supplementary material 2. Time sweep oscillatory test of 0A-100B dough at 1Hz and 25ºC.

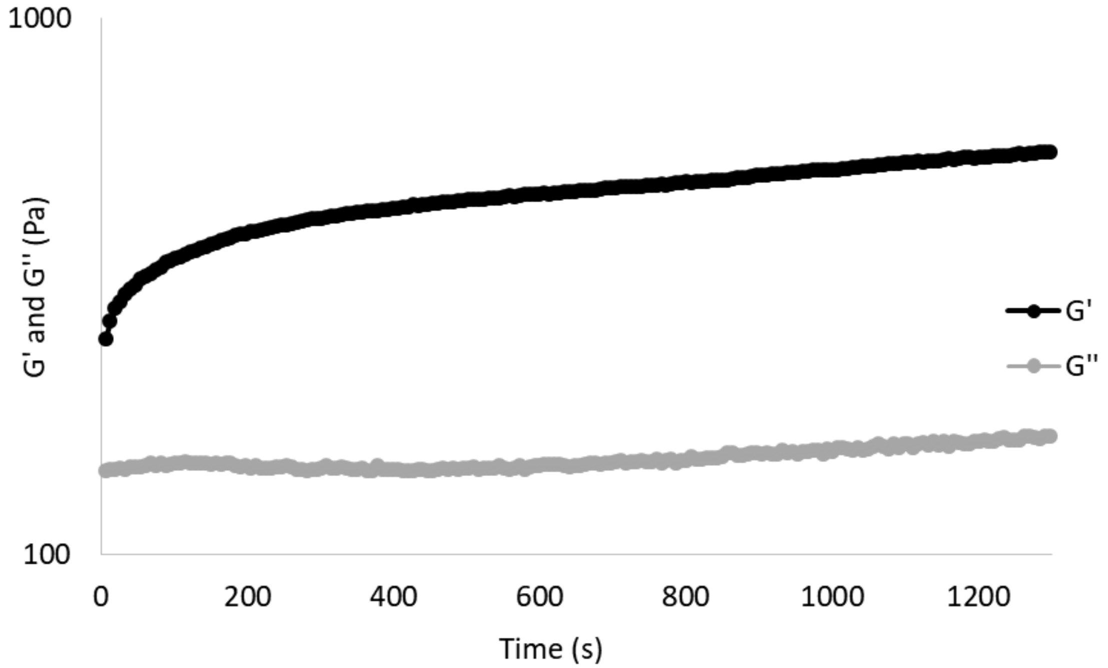

Supplementary material 3. Hot-stage microscopy videos of 100A-0B and 0A-100B doughs heated from 30 ºC to 100 ºC. Videos are available online.

Supplementary material 4. Gas production of doughs determined with a rheofermentometer.